METEOROLOGICAL APPLICATIONS
Meteorol. Appl. **23**: 158–164 (2016)
Published online 15 December 2015 in Wiley Online Library
(wileyonlinelibrary.com) DOI: 10.1002/met.1543

RMetS
Royal Meteorological Society

An empirical-analytical model of the vertical wind speed profile above and within an Amazon forest site

Cledenilson Mendonça de Souza,[a,b] Cléo Quaresma Dias-Júnior,[b,c]* Júlio Tóta[d] and Leonardo Deane de Abreu Sá[e]

[a] *Depart. de Zootecnia, Universidade Federal do Amazonas – UFAM, Parintins, Brasil*
[b] *CLIAMB, Instituto Nacional de Pesquisas da Amazônia – INPA, Manaus, Brasil*
[c] *Depart. de Física, Instituto Federal de Educação Ciência e Tecnologia do Pará – IFPA, Bragança, Brasil*
[d] *Depart. de Física, Universidade Federal do Oeste do Pará – UFOPA, Santarém, Brasil*
[e] *CRA, Instituto Nacional de Pesquisas Espaciais – INPE, Belém, Brasil*

ABSTRACT: The present study considers the mean wind velocity profiles measured from a 60 m high tower in the Rebio-Jarú forest (10° 04.7′ S, 61° 52.0′ W), located in the Brazilian northwestern state of Rondônia. The data were collected during the wet season as part of an intensive campaign of the large scale biosphere–atmosphere experiment in Amazonia. Nine cup anemometers were vertically placed to provide a good estimate of the inflection point height of the mean wind velocity profile. The resulting data were used to formulate a mean vertical wind speed profile, $\bar{u}(z)$, based on key parameters such as the inflection point height and the leaf area index. The modified hyperbolic tangent function was used to provide a more flexible fit to the experimental data. An exponential term was also added to the $\bar{u}(z)$ function, so that it can assume the appropriate 's' shape near the ground. Thus, some parameters were incorporated into the analytical profile function to enable more flexibility. The presented results demonstrate that the profile is a good fit to the experimental data measured above and within the Amazon forest canopy.

KEY WORDS wind profile; roughness sub-layer; modified hyperbolic tangent function; inflectional point; Amazon forest; turbulence

Received 16 January 2015; Revised 26 July 2015; Accepted 27 August 2015

1. Introduction

Previous investigations regarding the validity of similarity relationships in the atmospheric flow above tall forest canopies have noted some anomalous aspects of turbulent exchanges at the forest–atmosphere interface (Thom *et al.*, 1975). This raised interesting questions concerning the roughness sub-layer (RSL), which is present above very complex surfaces such as forests (Raupach and Thom, 1981; Cellier and Brunet, 1992; Finnigan, 2000). It is difficult to estimate the turbulent fluxes under such conditions (Sakai *et al.*, 2001; Von Randow *et al.*, 2002; Mahrt, 2010) and new similarity relationships are required (Raupach *et al.*, 1996; Marshall *et al.*, 2002; Sá and Pachêco, 2006). One important feature associated with these discrepancies is the existence of an inflection point in the mean wind profile. This generates a new kind of turbulent instability in the atmospheric flow because of the strong wind shear in the forest–atmosphere interface, which may create regions with 'like-roll' coherent vortices (Robinson, 1991; Raupach *et al.*, 1996). These vortices have peculiar spectral characteristics (Campanharo *et al.*, 2008; Dias-Júnior *et al.*, 2013), which may generate specific local phenomena such as spectral short-circuiting and turbulent wakes caused by the interaction of the forest canopy with the turbulent flow (Finnigan, 2000; Cava and Katul, 2008).

These complex flow characteristics make it difficult to estimate accurately the mean turbulent variables in the RSL near tall vegetation such as the Amazonian forest (Sakai *et al.*, 2001). Thus, it is important to determine the momentum transfer from the atmosphere to the surface when considering the role of the Amazonian forest in the biosphere–atmosphere exchanges. Problems related to the coupling between the atmospheric flow above and below the Amazon forest canopy were studied by Fitzjarrald *et al.* (1990), Viswanadham *et al.* (1990), Kruijt *et al.* (2000), Sá and Pachêco (2006) and Zeri *et al.* (2013), among others. Despite this extensive research, there are only a few systematic studies that associated the wind profile shapes with features of the Amazon forest canopy (such as foliage structure), as investigated by Yi (2008) for a forest in a temperate zone. These issues must be considered when developing surface–atmosphere exchange schemes for modelling purposes, which is the focus of the present study.

2. Materials and methods

2.1. Experimental site

The Rebio-Jarú forest reserve is located in the southwestern Amazon (0° 05′–10° 19′ S, 61° 35′–61° 57′ W). It is 2680 km^2 of typical tropical rain forest, ∼100–150 m above sea level (Zeri and Sa, 2010). A 60 m high micrometeorological tower was built in the Rebio-Jarú reserve (Figure 1). According to Andreae *et al.* (2002), the forest 'presents horizontally homogeneous conditions from northwest to southeast, which is the dominant wind direction (in a clockwise sense)'. McWilliam

* Correspondence: C. Q. Dias-Júnior, Instituto Federal de Educação Ciência e Tecnologia do Pará – IFPA, Rua da Escola Agrícola s/n, Bragança, PA 66400000, Brasil. E-mail: cleo.quaresma@ifpa.edu.br

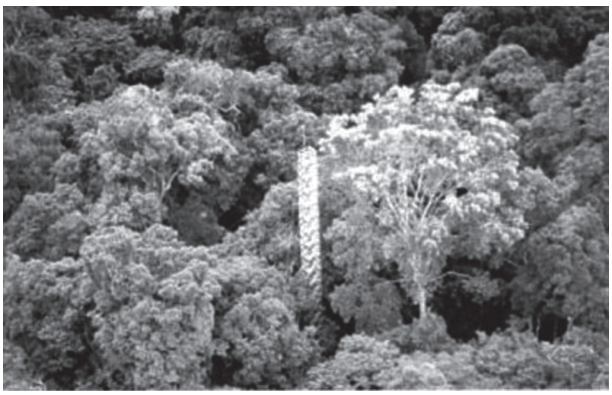

Figure 1. The micrometeorological tower built in the Rebio-Jarú reserve.

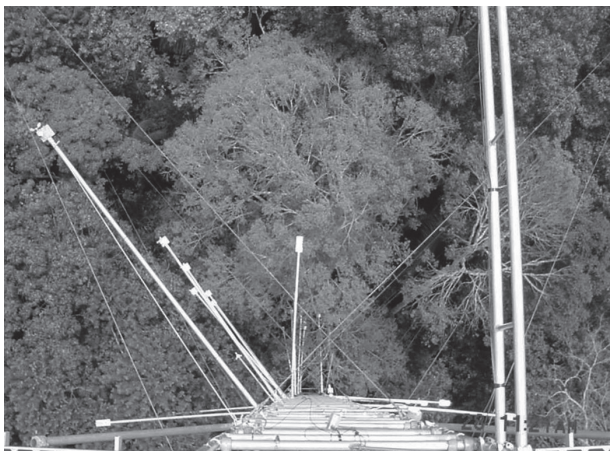

Figure 2. Profile of the nine cup anemometers installed in the Rebio-Jarú reserve's micrometeorological tower.

et al. (1996) presented information concerning the tree species found in this reserve. Culf *et al.* (1996), Andreae *et al.* (2002) and Dias-Júnior *et al.* (2013) presented several geographical and climatic reviews of this experimental site.

Several studies have considered the leaf area index (LAI) of Amazon forests, to estimate its value in different Amazonian experimental sites. Among them, Moura (2001) proposed an LAI of 6 for the Rebio-Jarú reserve, and Marques Filho *et al.* (2005) found LAI values of 6.4 and 6.1 for the Cuieiras Biological Reserve (also commonly referred to as ZF2) at km 14 and km 34 experimental sites, respectively. These sites are both located next to Manaus, in the central Amazon. Roberts *et al.* (1996) used different methods for estimating the LAI, and calculated values between 4.6 and 6 for the Rebio-Jarú reserve. Based on this result, this study used a LAI value of 6.

Some investigations suggest that there may be a relationship between the vertical wind profile and foliage structure. The findings of Yi (2008) imply that $\bar{u}(z)/\bar{u}_h$, is a function of LAI, where $\bar{u}(z)$ is the mean vertical wind speed profile and $\bar{u}_h$ is the mean wind speed at the top of the canopy. Doughty and Goulden (2008) analysed *in situ* and satellite data of the Tapajós National Forest in the Amazon, ∼150 km south of Santarém, Pará, Brazil. Their results showed that the LAI was subject to seasonal variations. According to these researchers, the LAI has a minimum value just over $4\,m^2\,m^{-2}$ from December through to April, a period that mostly corresponds to the local wet season. However, according to Doughty and Goulden (2008), leaf production increases from July to September, corresponding to the local dry season. During this period, many trees 'change their old leaves for new leaves', and the LAI may reach $6\,m^2\,m^{-2}$.

2.2. Dataset

The Rebio-Jarú reserve is one of the several experimental sites in the large scale biosphere–atmosphere (LBA) experiment in Amazonia. These extensive LBA experimental campaigns were carried out in two steps: the wet season campaign, from 25 January to 5 March 1999, and the dry-to-wet campaign, from 15 September to 10 November 2002 (Silva Dias *et al.*, 2002). As part of the scientific activities in the Rebio-Jarú reserve, the energy budget components, wind velocity, temperature and humidity were measured at several heights from a micrometeorological tower. Nine cup anemometers (Low Power A100L2, Vector Instruments Inc.) used for sampling at 0.1 Hz, provided the data for the wind profile, as shown in Figure 2. They were placed at previously defined levels to provide accurate information about the inflection point height, and useful information about the atmospheric flow in the forest–atmosphere interface. Thus, the instruments were installed vertically at heights of 55.00, 50.55, 47.70, 42.90, 40.25, 37.80, 32.85, 26.65 and 14.30 m.

Some of Vickers and Mahrt's (1997) procedures regarding quality control of the experimental data were applied to remove spurious spikes, amplitude resolution problems, dropouts and unrealistic data.

2.3. Theoretical elements and methodology

There is some experimental evidence that similarity relationships based on Monin–Obukhov similarity theory (MOST) cannot describe appropriately the atmospheric flow in the RSL above tall vegetation (Thom *et al.*, 1975; Cellier and Brunet, 1992; Raupach *et al.*, 1996; Finnigan, 2000; Py *et al.*, 2004). Many empirical formulations for normalized $\bar{u}(z)$ in the RSL have been proposed, based on the roughness parameters distinct of the well-known zero-plane displacement height (d) and roughness length (z_0). Such relationships can more appropriately express some exchange processes between the biosphere and the atmosphere that occur near the top of a tall forest (Raupach *et al.*, 1996; Finnigan, 2000; Marshall *et al.*, 2002; Py *et al.*, 2004; Sá and Pachêco, 2006; Doughty and Goulden, 2008; Tóta *et al.*, 2012; Dias-Júnior *et al.*, 2013).

Some significant issues associated with the wind profile's shape above the tall vegetation in the RSL are noted below.

1. Fitzjarrald *et al.* (1990) obtained some evidence that suggests that the flow in the canopy top provides information regarding a characteristic length scale (L_h) of the flow at the interface between the forest and the atmosphere. That is:

$$L_h = \frac{\overline{u}_h}{\left.\frac{\mathrm{d}\overline{u}}{\mathrm{d}z}\right|_h} \tag{1}$$

   where $\bar{u}_h$ is the mean wind velocity at level h (which corresponds to the mean canopy height) and $\left.\frac{\mathrm{d}\overline{u}}{\mathrm{d}z}\right|_h$ is the mean velocity gradient at h.
2. Raupach *et al.* (1996) used L_h to obtain a universal relationship that describes $\bar{u}(z)$ using the hyperbolic tangent function (HTF):

$$\frac{\overline{u}(z)}{\overline{u}_h} = 1 + \tanh\left(\frac{z}{L_h}\right) \tag{2}$$

3. Marshall *et al.* (2002) used wind tunnel data, and Sá and Pachêco (2006) used experimental data from the Amazon forest to investigate a formulation for $\bar{u}(z)$ that incorporates dynamical information of the inflection point height (z_i) and the wind shear measured at h. They used the scaling parameter u_i (mean wind velocity at z_i) as a characteristic velocity scale, and L_h as defined in Equation (1). Their analyses were extended to both flows, above and within the canopy. With these two characteristic scales, they obtained a general relationship for the vertical profile:

$$\overline{u}/u_i = F\left[\left(z - z_i\right)/L_h\right] \tag{3}$$

where $\bar{u}$ is the mean wind velocity at z, and F is a function whose mathematical form is determined empirically from experimental data. This fits very well with the experimental data measured far above the ground, but does not explain the influence of the canopy's foliage structure on the shape of the wind profile. To overcome this drawback, a new modified HTF formulation was proposed, which was based on earlier models of vertical wind profiles in the RSL (Raupach *et al.*, 1996; Yi, 2008). A mathematical device was added to the $\bar{u}(z)$ function to obtain a better fit for this curve.

The theoretical bases for this proposition were presented by Raupach *et al.* (1996), who considered an inflection point on the vertical wind profile next to the top of the canopy. They suggested that the HTF can provide a good numerical fit to the vertical wind profile data. However, a simple HTF cannot generate a good numerical fit, if the actual empirical function for $\bar{u}(z)$ is not exactly symmetrical with respect to z_i. Thus, a modified form of the HTF is proposed to improve the fit of $\bar{u}(z)$, which can more flexibly incorporate asymmetric shapes. This technique can provide: (1) a good analytical model for the wind speed profile, which results in a good experimental fit for the regions above and below z_i, and (2) a new formulation for $\bar{u}(z)$, which incorporates some features of the vertical structure of the forest canopy and some aerodynamic characteristics of the coupling between the flows above and within the canopy. The best-fitting curve is not perfectly anti-symmetric with respect to the horizontal axis at z_i. Therefore, to improve this fit, some flexible features were inserted into the best-fitting curve, making it less rigid than the original HTF. For this, a new argument is proposed for the HTF. Following on from the HTF model formulations of Raupach *et al.* (1996) and Yi (2008), this leads to a new formulation for $\bar{u}(z)$ above and within the forest canopy:

$$\overline{u}(z) = \overline{u}_H\left\{\tanh\left[\beta + \gamma\exp\left(-\mathrm{LAI}\left(1 - {}^{z}/_{z_i}\right)\right)\right]\right\} \tag{4}$$

where H is the height of the highest measuring level (55 m, for the Rebio-Jarú experimental site); $\bar{u}_H$ is the mean wind speed at the H; β and γ are fitting parameters; z_i is the inflection point height of the vertical wind profile; z is a measuring height; and $\bar{u}(z)$ is the mean wind speed at z. Here β and γ are new parameters, which are explained as follows.

The parameter β influences the lower wind profile. That is, it can change the wind profile within the forest canopy. This is mainly useful for wind profiles in regions where there is a secondary maximum in the wind profile, due to the trunk spaces of forests (Kaimal and Finnigan, 1994, pp. 77–79). In the Amazon forests, such occurrences of secondary maximums in the wind profiles can exist in forests located in slopes or valleys. For example, the forests studied by Araújo *et al.* (2010) and Tóta *et al.* (2012) in their investigations regarding the effects of terrain heterogeneity on atmospheric flows within tall vegetation. The β parameter provides a best fit to the wind profile in these situations.

The parameter γ influences the wind profile in the opposite way to β, that is, it amplifies the upper part of the wind profile without introducing substantial changes to the lower part. The γ parameter can describe the wind profile's shape over forests located in horizontally homogeneous, smooth areas, where drainage flows or secondary maxima are not expected. In these situations, the forests' LAIs are sufficiently high to hamper momentum transport deep into the canopy.

To improve the profile fit, and to allow for an 's' shape near the ground (as suggested by Yi (2008)), an exponential term was included in the analytical form of $\bar{u}(z)$:

$$\overline{u}(z) = \overline{u}_H\left\{\left[\frac{-1+\exp(\mu z)}{\exp(\omega z)}\right]\alpha\tanh\left[\beta + \gamma \times\exp\left(-\mathrm{LAI}\left(1 - \frac{z}{z_i}\right)\right)\right]\right\} \tag{5}$$

where μ, α, β , γ and ω are fit parameters and LAI = 6 for the Rebio-Jarú forest (Moura, 2001). Also α, μ and ω are new parameters, and are described as follows.

The parameter α multiplies the entire second part of Equation (5), which describes the dimensionless vertical profile of the wind speed above and within the forest canopy. Thus, it should produce a better fit to the vertical wind profile, covering conditions ranging from very light winds to strong winds. In summary, α is strongly correlated with the average wind speed at any time.

The parameters μ and ω enable more flexibility in terms of the s-shaped region located below $z = 20$ m. They do not influence the z_i value in the superior part of $\bar{u}(z)$. Thus, these parameters may incorporate some of the mechanical effects of the vegetation roughness and buoyancy effects. They are intended to make z dimensionless within the two arguments of the exponential functions in Equation 5 (but not in Equation (4)). They are generally close to unity (i.e. 1). However, the arguments are within the exponential functions, so they can introduce considerable variations in the dimensionless wind profile. These parameters may be considered as a single constant in this study. In the Rebio-Jarú tower, the wind velocities were recorded down to $z = 14$ m.

3. Results

The first numerical experiment analysed the wind speed profiles provided by Equation (4). The curves generated by this model and by experimental data are presented in Figure 3. They depict shapes that are not completely symmetric with respect to the inflection point. The variables in Figure 3 are not dimensionless. Thus, this model was not built with the aim of obtaining universal relationships, but simply to show the mean shape of the wind field under a wide range of environmental conditions.

The β and γ parameters in Equation (4) are linked to the physical effects acting on and above the inflectional point zone. These parameters are associated with the existence of a roughness sublayer (Finnigan, 2000), its heterogeneous features resulting from the effect of distinct canopy architectures on the turbulence structure (Baldocchi and Meyers, 1988), and its prevailing atmospheric stability conditions (Mahrt *et al.*, 2001). Figures 4 and 5 help to explain the physical meanings of β and γ. Figure 4 shows that variations in β change the inferior part of the curve representing the lower canopy region. In contrast, Figure 5 shows how variations in γ change the behaviour of the curve in the region near the canopy.

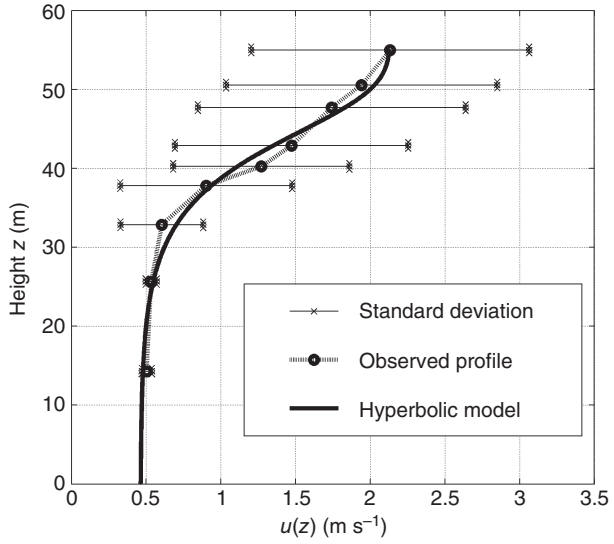

Figure 3. The observed mean vertical wind profile compared with the hyperbolic tangent function (HTF) model (15 February 1999; 0800 to 0900 LST (1200 to 1300 UTC).

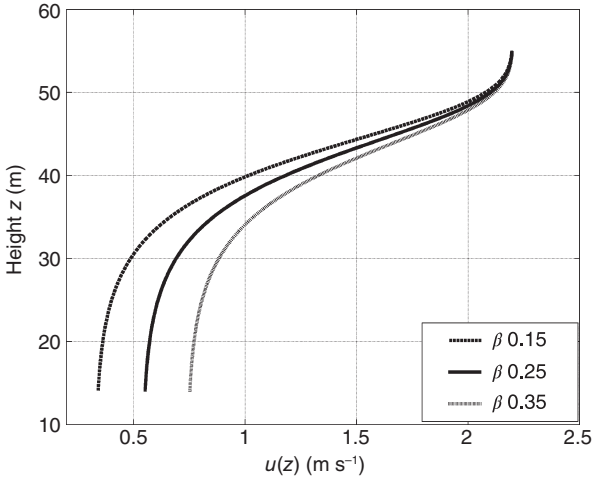

Figure 4. Modelled wind profiles for different values of β.

Dias-Júnior *et al.* (2013) recently found that the z_i values observed above the Rebio-Jarú reserve varied over the daytime. They found that z_i tends towards a maximum value of 41 m in the early morning and the late afternoon. However, at noon, it falls to ∼38 m, as shown in Figure 6.

These z_i values were used to test how well the modified HTF model fits $\bar{u}(z)$. Thus, the function for $\bar{u}(z)$ in Equation (4) was used to calculate the hourly wind profile data for 13 February 1999 under two conditions: (1) z_i varied according to the Dias-Júnior procedure, and (2) fixed z_i.

These results indicate that the best fits for $\bar{u}(z)$ were obtained when: (1) β had a fixed value of 0.13 (which was obtained after many empirical tests), and (2) z_i and γ varied over the daytime. Parameter z_i incorporates the asymmetrical effect in $\bar{u}(z)$. Physically, it expresses the influence of the canopy top forcing on a vortex centred on z_i (Raupach *et al.*, 1996). In contrast, γ has a similar daytime trend to z_i, as shown in Figure 6.

To compare the observed and modelled profiles, i.e. $\bar{u}(z)$, data from 13 February 1999 were used to calculate the correlation co-efficients for each z. These were then used to estimate a mean correlation co-efficient, r (Table 1). The results were calculated

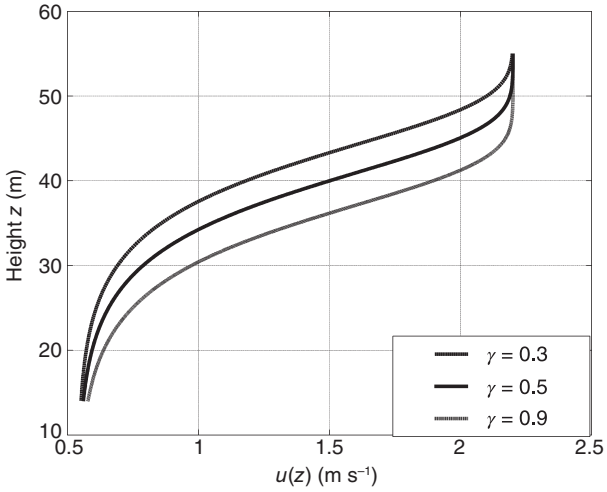

Figure 5. Modelled wind profiles for different values of γ.

for two conditions, to investigate variations to the wind profile shape over the daytime. In condition r_1, the values of z_i varied, and in r_2 the values of z_i are held fixed (=41 m). It is observed that $r_1 > r_2$, an indication that the wind speed profile was better modelled for the situations in which z_i was considered as being a variable parameter.

To investigate the physical role of each of these fit parameters, Figure 7 contains plots of $\bar{u}(z)$ *versus* z, where only one parameter was varied in each subplot. Figure 7(a) shows the wind profiles for different values of α. It amplifies the wind speed values as a whole. Figure 7(b) shows the wind profiles for different values of β. These profiles have the same wind speed value at the highest measurement. The differences between the two groups of wind profiles are more pronounced in the region corresponding to the within-canopy zone. Figure 7(c) shows wind profiles for different values of γ. There is the same split in wind speed values as in Figure 7(b). However, unlike the previous figure, this split is more pronounced in the higher part of the profile. Figure 7(d) presents wind profiles for different values of μ. The wind profile shapes in Figure 7(a) and (d) are quite similar, except in the region immediately above the ground, where the profiles in Figure 7(d) slowly converge to the same curve (unlike in Figure 7(a)). The wind profile is very sensitive to changes in ω. Small variations can generate significant distortions in the wind profile, as shown in Figure 7(e). The LAI parameter has a marked influence on the wind profile shape. When LAI is relatively small, the wind profile loses its s-shape, as shown in Figure 7(f).

According to Doughty and Goulden (2008), the information provided by Equation (4) and the seasonal variability of LAI suggest that the vertical wind profile also undergoes seasonal changes. This can be seen in Figure 8, which contains two modelled profiles generated using the $\bar{u}(z)$ function, one for LAI = 4.2 and the other for LAI = 5.8. In this figure, $\bar{u}_h$ = 2.2 m s^{-1}, β = 0.25, γ = 0.5 and z_i = 39 m. These values are similar to those found by Doughty and Goulden (2008) for the minimum and maximum LAIs in the Amazon forest. Figure 8 shows the differences between the $\partial\bar{u}/\partial z$ values at level z_i for the curves representing dry and wet periods. In the wet period, $\partial\bar{u}/\partial z$ in the region immediately above the canopy is greater than during the dry season. Consequently, it is more difficult for the atmospheric flow to transfer momentum into the canopy during the wet season than during the dry season, as expected.

There is another indication of a possible seasonal LAI variability in the Amazon forest, and of its consequences concerning the

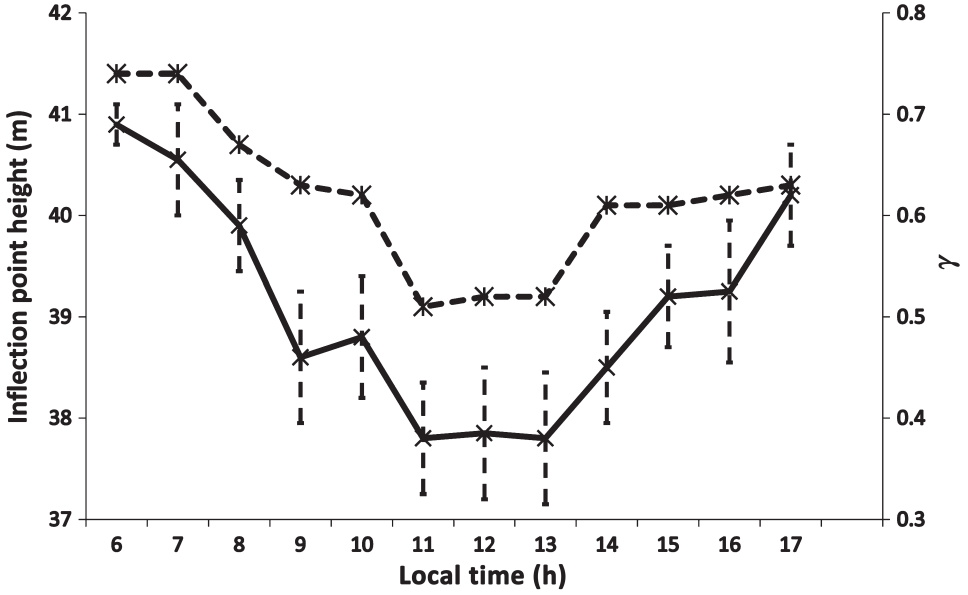

Figure 6. Daytime hourly variation of inflection point height (solid line) and γ values (dashed line) for the Rebio-Jarú reserve.

Table 1. Daytime hourly variation of the correlation co-efficients r_1 and r_2 measured in the Rebio-Jarú reserve for 13 March 1999.

Hour (LST)	r_1 (z_i variable)	r_2 ($z_i = z$ 41 m)
0600	0.989	0.989
0700	0.986	0.985
0800	0.996	0.993
0900	0.989	0.976
1000	0.983	0.971
1100	0.983	0.961
1200	0.983	0.957
1300	0.987	0.967
1400	0.990	0.973
1500	0.986	0.976
1600	0.989	0.981
1700	0.991	0.990

surface drag imposed by the plant canopy on the immediately above atmospheric flow. Mafra (2014) analysed the seasonal variability of nocturnal turbulent regimes above the Amazon forest in the Uatumã experimental site (central Amazon), using the methodology proposed by Sun *et al.* (2012) who found different values for the threshold value (V_L) of the average wind speed above the forest canopy that separates the weak and strong turbulence regimes. The physical processes behind this threshold have recently received much attention (Martins *et al.*, 2013; Mafra, 2014; Andreae *et al.*, 2015), and the associated physical transition process was designated as a 'HOST' (hockey-stick transition) by Sun *et al.* (2015).

The β and γ parameters inside the HTF argument are linked to physical effects, which occur at the inflection point zone and above. They are probably associated to the existence of the roughness sublayer, and the so called mixing-layer analogy (Raupach *et al.*, 1996), which states that the wind speed profile

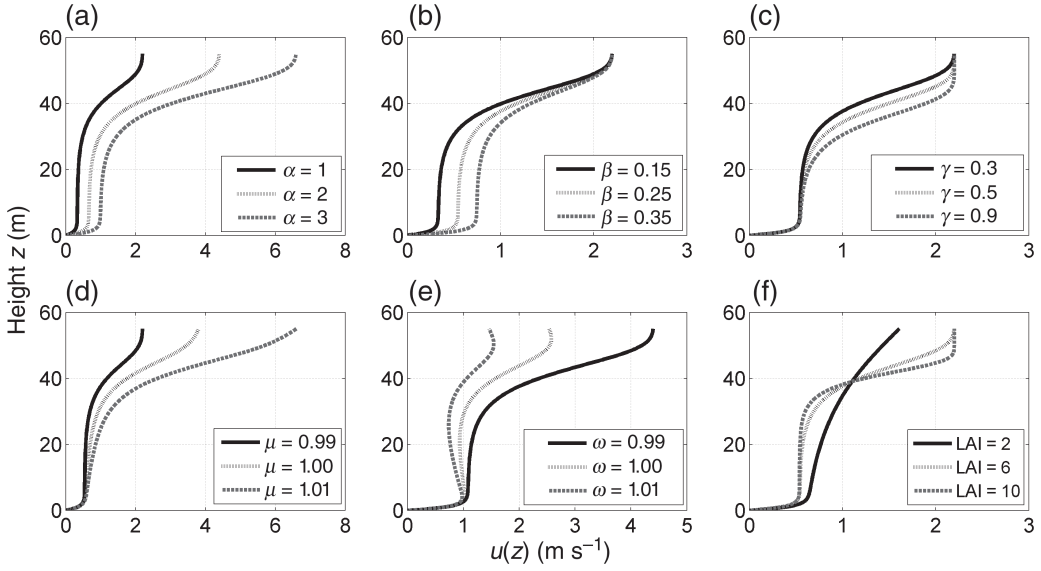

Figure 7. Modelled wind profiles for different parameter values: (a) α; (b) β; (c) γ; (d) μ; (e) ω; and (e) leaf area index (LAI).

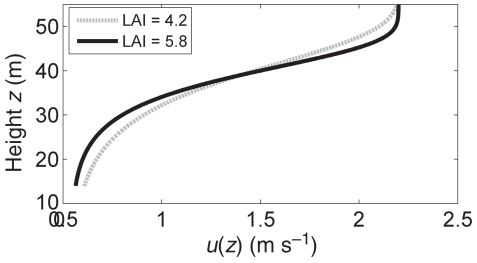

Figure 8. Modelled wind profiles for two different values of leaf area index (LAI) (4.2, dashed grey line and 5.8, black solid line), which correspond to the seasonal extreme values in the Amazon forest.

above tall vegetation has an inflection point. This suggests that the region separates into two flow layers with distinct velocities, in which a turbulent vortex is expected, or, in the words of Cava and Katul (2008), a 'dominant eddy'. This vortex could also be associated with the organization of 'rolls' in the atmospheric flow with respect to rotation axes transverse to the mean stream direction (Robinson, 1991). However, according to Dias-Júnior *et al.* (2013), the height of the wind profile inflection point varies throughout the day. During the night, when the wind speed is sufficiently strong above the Rebio-Jarú, z_i increases creating conditions that allow the dominant eddy to penetrate more strongly and deeply into the canopy (higher torque associated with the vortex). This generates a more effective exchange of energy and mass between the regions above and within the forest canopy (Dias-Júnior *et al.*, 2013). At night, this process is associated with situations where the average wind speed exceeds the V_L for a 'HOST' phenomenon (Sun *et al.*, 2015). This increases the effectiveness of the mixture in the forest–atmosphere interface, challenging the traditional flux-profile relationships of HOST (Sun *et al.*, 2015).

Figure 9 shows an abstract generalization of Figure 3, incorporating the features of a hypothetical secondary maximum in the wind profile. This secondary maximum is sometimes found in the trunk spaces of forests (Baldocchi and Meyers, 1988; Kaimal and Finnigan, 1994, pp. 77–79). Thus, the lower part of Figure 9 refers to a hypothetical analytical form of the function $\bar{u}(z)/\bar{u}_h(z)$ near the forest floor. This, when incorporated into Equation (4) (the HTF) results in Equation (5) (the so called modified HTF). Figure 9 shows that the mean wind speed profile fits very well with the data.

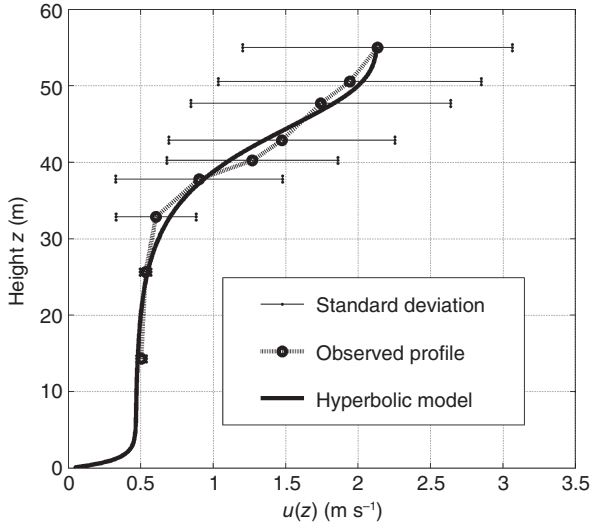

Figure 9. Observed mean wind profile and associated standard deviation compared with the hyperbolic tangent function (HTF) fitted data (second version).

4. Conclusions

The present study proposes an empirical-analytical model for describing the vertical wind speed profile above and within an Amazon forest, and provides a general non-dimensional relationship. The hyperbolic tangent function was modified to obtain a better fit to the experimental data collected above and within the Amazon forest. This function provides a good fit in many experimental situations, where there is variation in the height of the inflection point of the vertical wind speed profile. These results are mainly useful for two reasons. First, they can be used to obtain a realistic estimate of the vertical wind profile when there is a limited amount of data. Second, they provide useful information regarding modifications to the wind profile shape introduced by several distinct conditions. These include changes to the leaf area index values and changes to the height of the vertical profile's inflectional point. This formulation provides a better fit to the experimental data measured above and within the Amazon forest canopy.

Acknowledgments

The authors would like to thank all those directly or indirectly contributed to the fulfilment of the 1999 LBA – Intensive wet Campaign, and the support of the university in Ji-Paraná (UNIR), Instituto Brasileiro do Meio Ambiente e dos Recursos Naturais Renováveis (IBAMA) and Instituto Nacional de Colonização e Reforma Agrária (INCRA). This work was done under the LBA project framework, sponsored by the European Union, NASA, and Brazilian Agencies as the Conselho Nacional de Pesquisa e Desenvolvimento Tecnológico (CNPq) and the Fundação de Amparo a Pesquisa do Estado de São Paulo (FAPESP, process 01/06908-7). Leonardo Sá is particularly grateful to CNPq for his research grant (process303.728/2010-8).

References

Andreae MO, Acevedo OC, Araùjo A, Artaxo P, Barbosa CGG, Barbosa HMJ, et al. 2015. The Amazon Tall Tower Observatory (ATTO): overview of pilot measurements on ecosystem ecology, meteorology, trace gases, and aerosols. *Atmos. Chem. Phys.* **15**: 10723–10776.

Andreae MO, Artaxo P, Brandão C, Carswell FE, Ciccioli P, Costa AL, et al. 2002. Biogeochemical cycling of carbon, water, energy, trace gases, and aerosols in Amazonia: the LBA-EUSTACH experiments. *J. Geophys. Res.* **33**: 1–25.

Araújo AC, Dolman AJ, Waterloo MJ, Gash JHC, Kruijt B, Zanchi FB, et al. 2010. The spatial variability of CO_2 storage and the interpretation of eddy covariance fluxes in central Amazonia. *Agric. For. Meteorol.* **150**: 226–237.

Baldocchi DD, Meyers TP. 1988. Turbulence structure in a deciduous forest. *Bound.-Layer Meteorol.* **43**(4): 345–364.

Campanharo ASLO, Ramos FM, Macau EEN, Rosa RR, Bolzan MJA, Sa LDA. 2008. Searching chaos and coherent structures in the atmospheric turbulence above Amazon forest. *Philos. Trans. R. Soc. A* **366**: 579–589.

Cava D, Katul GG. 2008. Spectral short-circuiting and wake production within the canopy trunk space of an alpine hardwood forest. *Bound.-Layer Meteorol.* **126**: 415–431.

Cellier P, Brunet Y. 1992. Flux-gradient relationships above tall plant canopies. *Agric. For. Meteorol.* **58**: 93–117.

Culf AD, Esteves JL, Marques Filho AO, Rocha HR. 1996. Radiation, temperature and humidity over forest and pasture in Amazonia. In

Amazonian Deforestation and Climate, Gash JHC, Nobre CA, Roberts JM, Victoria RL (eds). Wiley: Chichester; 175–191.
Dias-Júnior CQ, Sá LDA, Pachêco VB, Souza CM. 2013. Coherent structures detected in the unstable atmospheric surface layer above the Amazon Forest. *J. Wind Eng. Ind. Aerodyn.* **115**: 1–8.
Doughty CE, Goulden ML. 2008. Seasonal patterns of tropical forest leaf area index and CO_2 exchange. *J. Geophys. Res.* **113**: G00B06.
Finnigan JJ. 2000. Turbulence in plant canopies. *Annu. Rev. Fluid Mech.* **32**: 519–571.
Fitzjarrald DR, Moore KE, Cabral OMR, Scolar J, Manzi AO, Sá LDA. 1990. Daytime turbulent exchange between the Amazon forest and the atmosphere. *J. Geophys. Res.* **95**: 16825–16838.
Kaimal JC, Finnigan JJ. 1994. *Atmospheric Boundary Layer Flows. Their Structure and Measurement*. Oxford University Press: New York, NY,; 289.
Kruijt B, Malhi Y, Lloyd J, Norbre AD, Miranda AC, Pereira MGP, et al. 2000. Turbulence statistics above and within two Amazon rain forest canopies. *Bound.-Layer Meteorol.* **94**: 297–331.
McWilliam ALC, Cabral OMR, Gomes BM, Esteves JL, Roberts JM. 1996. Forest and pasture leaf-gas exchange in south-west Amazonia. In *Amazonian Deforestation and Climate*, Gash JHC, Nobre CA, Roberts JM, Victoria RL (eds). Wiley; 265–285.
Mafra ACB. 2014. Características das trocas turbulentas noturnas de CO_2 entre a floresta de Uatumã, Amazonas, e a atmosfera, Dissertação de Mestrado em Ciências Ambientais, Universidade Federal do Pará, Belém, Pará, Brazil.
Mahrt L. 2010. Computing turbulent fluxes near the surface: needed improvements. *Agric. For. Meteorol.* **150**: 501–509.
Mahrt L, Vickers D, Sun J, Jensen NO, Jorgensen H, Pardyjak E, et al. 2001. Determination of the surface drag coefficient. *Bound.-Layer Meteorol.* **99**: 249–276.
Marques Filho AO, Dallarosa RG, Pachêco VB. 2005. Radiação solar e distribuição vertical de área foliar em floresta – Reserva Biológica do Cuieiras – ZF2, Manaus. *Acta Amazonia* **35**(4): 427–436.
Marshall BJ, Wood CJ, Gardiner BA, Belcher BE. 2002. Conditional sampling of forest canopy gusts. *Bound.-Layer Meteorol* **102**: 225–251.
Martins HS, Sá LDA, Moraes OLL. 2013. Low level jets in the Pantanal wetland nocturnal boundary layer – case studies. *Am. J. Environ. Energy* **3**(1): 32–47.
Moura RG. 2001. A study of the solar and terrestrial radiation above and inside a tropical rain forest, MSc thesis in Meteorology, National Institute of Space Research, Brazil (INPE-14015-TDI/1194).
Py C, de Langre E, Moulia B. 2004. The mixing layer instability of wind over a flexible crop canopy. *C. R. Mecan.* **332**: 613–618.
Raupach MR, Finnigan JJ, Brunet Y. 1996. Coherent eddies and turbulence in vegetation canopies: the mixing-layer analogy. *Bound.-Layer Meteorol.* **78**: 351–382.
Raupach MR, Thom AS. 1981. Turbulence in and above plant canopies. *Annu. Rev. Fluid Mech.* **13**: 97–129.
Roberts JM, Cabral OMR, McWilliam A-LC, da Costa J d P, Sá TD d A. 1996. An overview of the leaf area index and physiological measurements during ABRACOS. In *Amazonian Deforestation and Climate*, Gash JHC, Nobre CA, Roberts JM, Victoria RL (eds). Wiley: Chichester; 287–306.
Robinson SK. 1991. Coherent motions in the turbulent boundary layer. *Annu. Rev. Fluid Mech.* **23**: 601–639.
Sá LDA, Pachêco VB. 2006. Wind velocity above and inside Amazonian rain forest in Rondonia. *Rev. Bras. Meteorol.* **21**: 50–58.
Sakai RK, Fitzjarrald DR, Moore KE. 2001. Importance of low-frequency contributions to eddy fluxes observed over rough surfaces. *J. Appl. Meteorol.* **40**: 2178–2192.
Silva Dias MAFS, Rutledge S, Kabat P, Silva Dias P, Nobre C, Fisch G, et al. 2002. Clouds and rain processes in a biosphere atmosphere interaction context in the Amazon Region. *J. Geophys. Res.* **107**: 8072.
Sun J, Mahrt L, Banta RM, Pichugina YL. 2012. Turbulence regimes and turbulence intermittency in the stable boundary layer during CASES-99. *J. Atmos. Sci.* **69**: 338–351.
Sun J, Mahrt L, Nappo C, Lenschow DH. 2015. Wind and temperature oscillations generated by wave-turbulence interactions in the stably stratified boundary layer. *J. Atmos. Sci.* **72**: 1484–1503.
Thom AS, Stewart JB, Oliver HR, Gash JHC. 1975. Comparison of aerodynamic and energy budget estimates of fluxes over a pine forest. *Q. J. R. Meteorol. Soc.* **101**: 93–105.
Tóta J, Fitzjarrald DR, Silva Dias MAF. 2012. Amazon rainforest exchange of carbon and subcanopy air flow: Manaus LBA site – a complex terrain condition. *Sci. World J.* **2012**: 165067, DOI: 10.1100/2012/165067.
Vickers D, Mahrt L. 1997. Quality control and flux sampling problems for tower and aircraft data. *J. Atmos. Oceanic Technol.* **14**(3): 512–526.
Viswanadham Y, Molion LCB, Manzi AO, Sá LDA, Silva Filho VP, André RGB, et al. 1990. Micrometeorological measurements in Amazon forest during GTE-ABLE-2A mission. *J. Geophys. Res.* **95**: 13669–13682.
von Randow C, Sá LDA, Gannabathula PS, Manzi AO, Arlino PR, Kruijt B. 2002. Scale variability of atmospheric surface layer fluxes of energy and carbon over a tropical rain forest in southwest Amazonia 1. Diurnal conditions. *J. Geophys. Res.-Atmos.* **107**(D20): LBA-29-1–LBA-29-12.
Yi C. 2008. Momentum transfer within canopies. *J. Appl. Meteorol. Climatol.* **47**: 262–275.
Zeri M, Sa LDA. 2010. The impact of data gaps and quality control filtering on the balances of energy and carbon for a South west Amazon forest. *Agric. For. Meteorol.* **150**: 1543–1552.
Zeri M, Sá LDA, Nobre CA. 2013. Estimating buoyancy heat flux using the surface renewal technique over four Amazonian forest sites in Brazil. *Bound.-Layer meteorol.* **149**(2): 179–196.

